

In the format provided by the authors and unedited.

# Ultrastable low-bias water splitting photoanodes via photocorrosion inhibition and *in situ* catalyst regeneration

Yongbo Kuang,<sup>1,2</sup> Qingxin Jia,<sup>1,2</sup> Guijun Ma,<sup>1,2</sup> Takashi Hisatomi,<sup>1,2</sup> Tsutomu Minegishi,<sup>1,2</sup>  
Hiroshi Nishiyama,<sup>1,2</sup> Mamiko Nakabayashi,<sup>2,3</sup> Naoya Shibata,<sup>3</sup> Taro Yamada,<sup>1,2</sup> Akihiko  
Kudo,<sup>2,4</sup> Kazunari Domen\*<sup>1,2</sup>

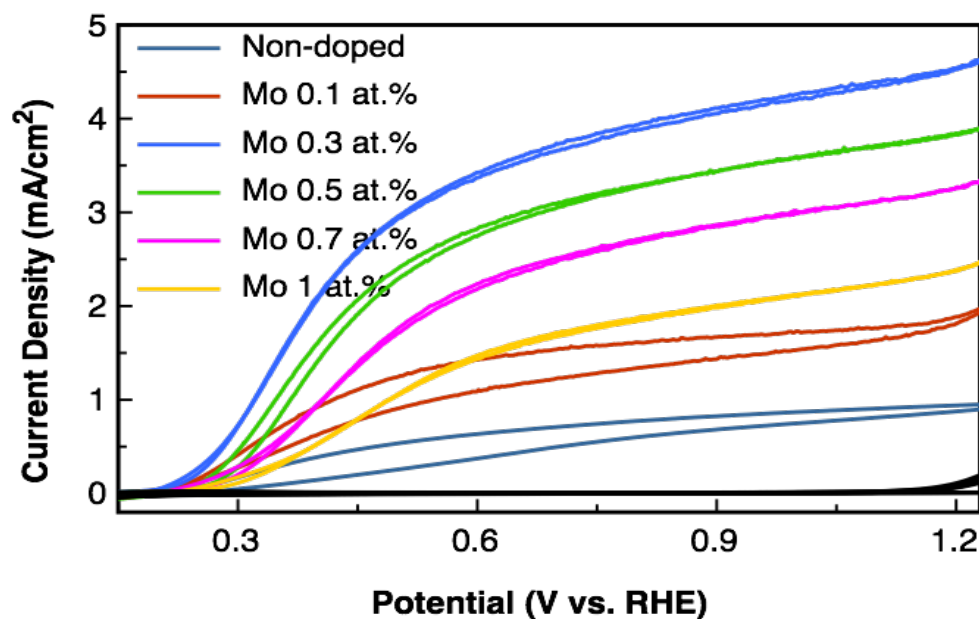
<sup>1</sup>Department of Chemical System Engineering School of Engineering, The University of Tokyo, 7-3-1 Hongo, Bunkyo-ku, Tokyo 113-8656, Japan.

<sup>2</sup>Japan Technological Research Association of Artificial Photosynthetic Chemical Process (ARPCChem), 7-3-1 Hongo, Bunkyo-ku, Tokyo 113-8656, Japan.

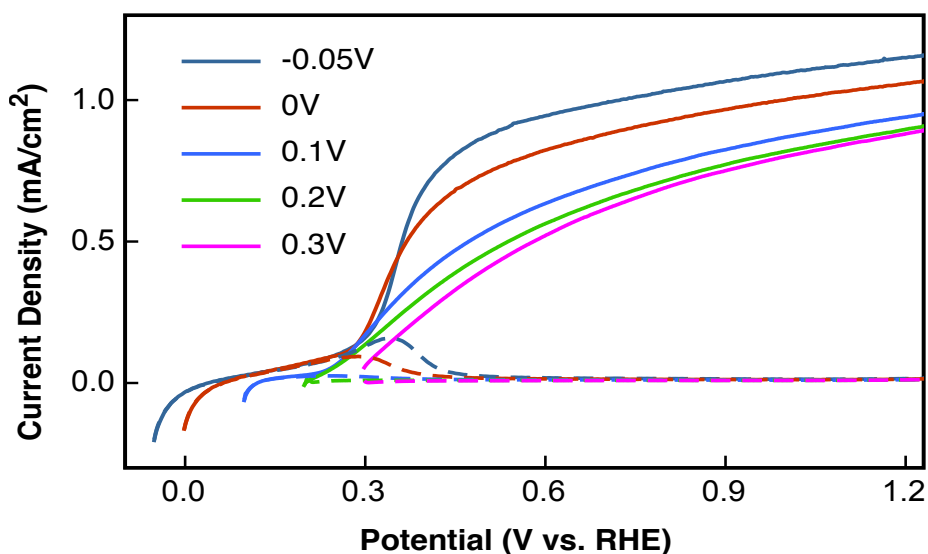
<sup>3</sup>Institute of Engineering Innovation, The University of Tokyo, 2-11-16 Yayoi, Bunkyo-ku, Tokyo 113-8656, Japan.

<sup>4</sup>Department of Applied Chemistry Faculty of Science, Science University of Tokyo, 1-3 Kagurazaka, Shinjuku-ku, Tokyo 162-8601, Japan.

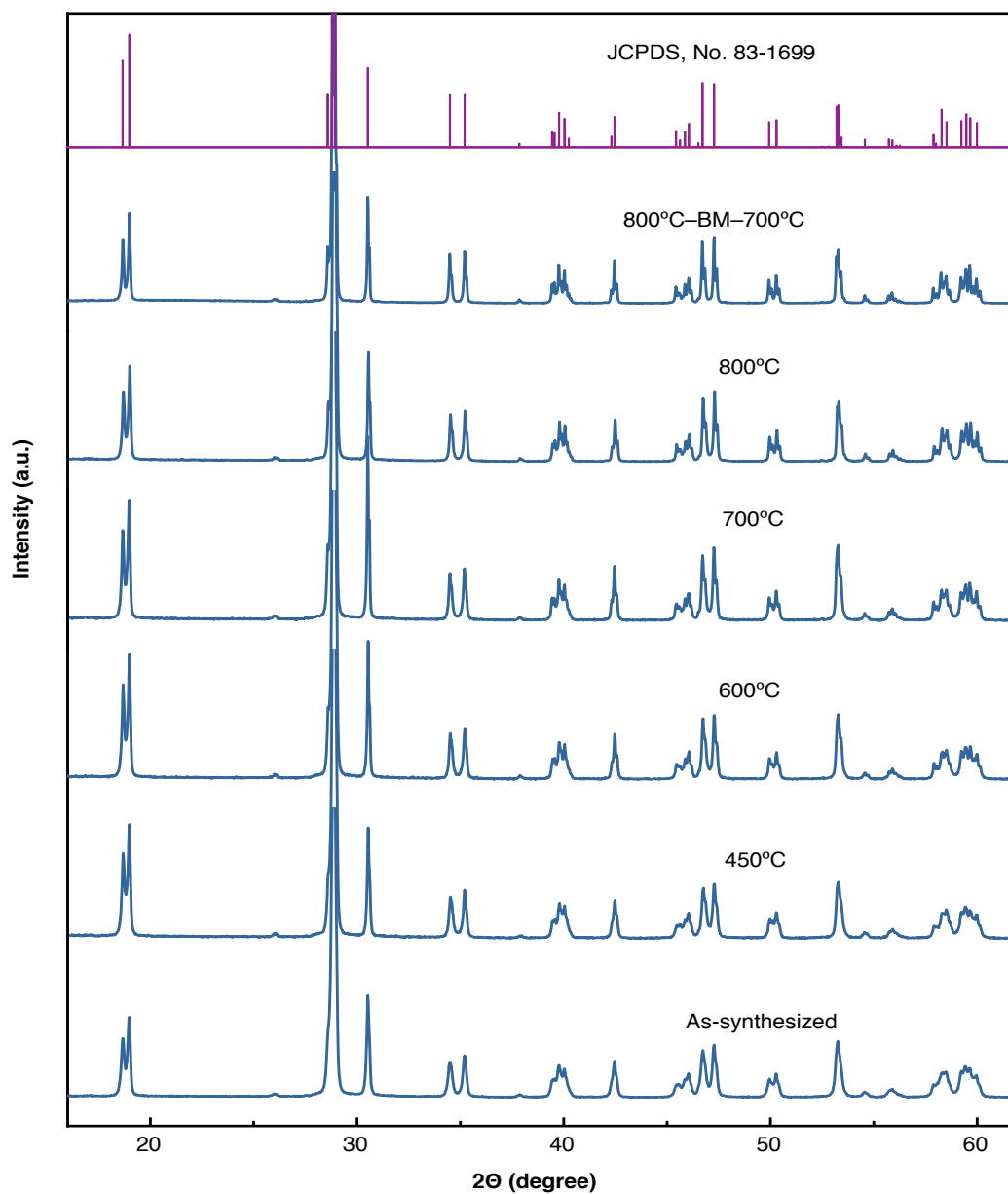
\*E-mail: [domen@chemsys.t.u-tokyo.ac.jp](mailto:domen@chemsys.t.u-tokyo.ac.jp)



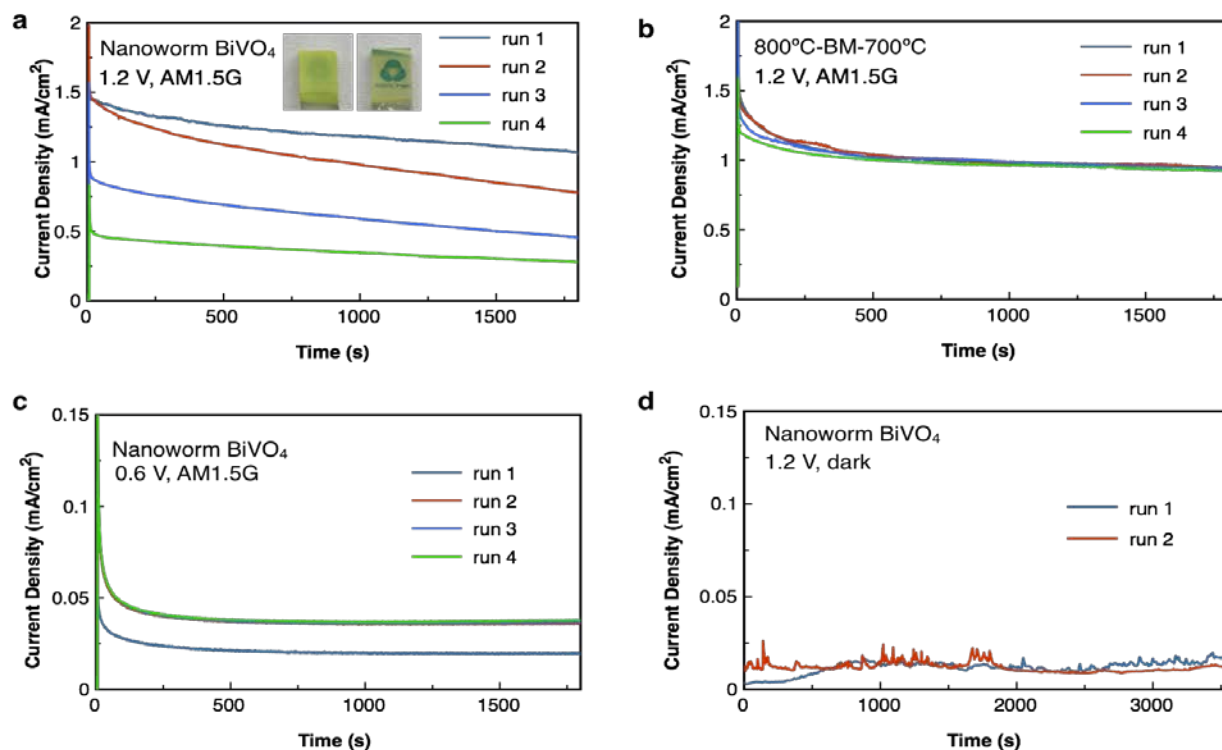
Supplementary Figure 1 | Effect of Mo-doping contents on the photoelectrochemical properties of bare Mo:BiVO<sub>4</sub>/Ni/Sn electrodes. CV curves of BiVO<sub>4</sub> particle electrodes prepared from particles with Mo doping concentrations between 0-1 at.% were recorded for sulphite oxidation under AM1.5G irradiation. The black curves are the corresponding dark currents. All BiVO<sub>4</sub> particles were treated by 800 °C annealing, ball milling and 700 °C post annealing sequentially. The photocurrent decreased for samples over-doped with Mo, which presumably also behaves as sites for charge recombination. Hysteresis curves are found for 0 at.% and 0.1 at.% Mo-doped samples, which might be associated with V<sup>5+</sup>/V<sup>4+</sup> redox and the population of O vacancy. Further confirmation can be found in Supplementary Figure 4, which shows the dependence of photocurrents on the reduction history of a non-doped BiVO<sub>4</sub> electrode.



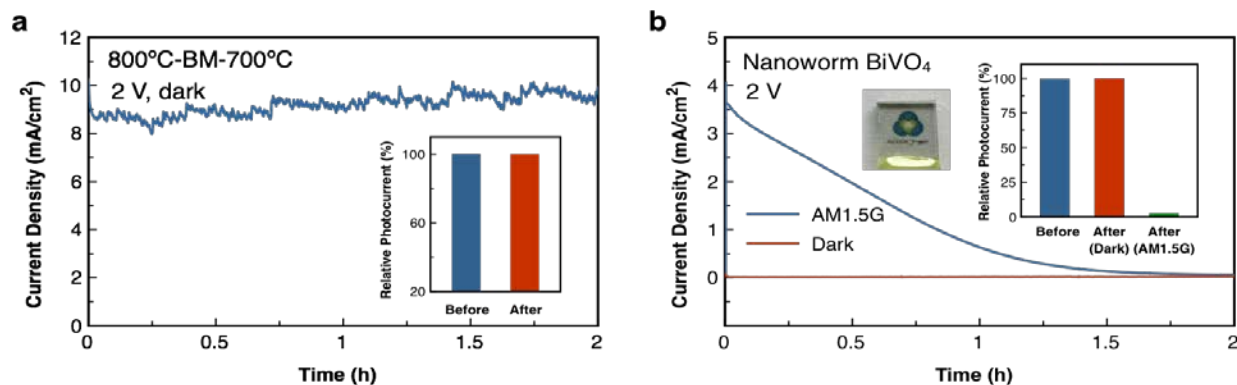
Supplementary Figure 2 | The effect of redox history on PEC performance of non-doped BiVO<sub>4</sub> electrode. The non-doped BiVO<sub>4</sub> powder was treated by 800 °C annealing, ball milling and 700 °C post annealing sequentially. J-V curves were measured with different starting applied potentials, in the order of increasing starting applied potential, for sulphite oxidation under AM 1.5G irradiation. Dashed curves were measured in dark.



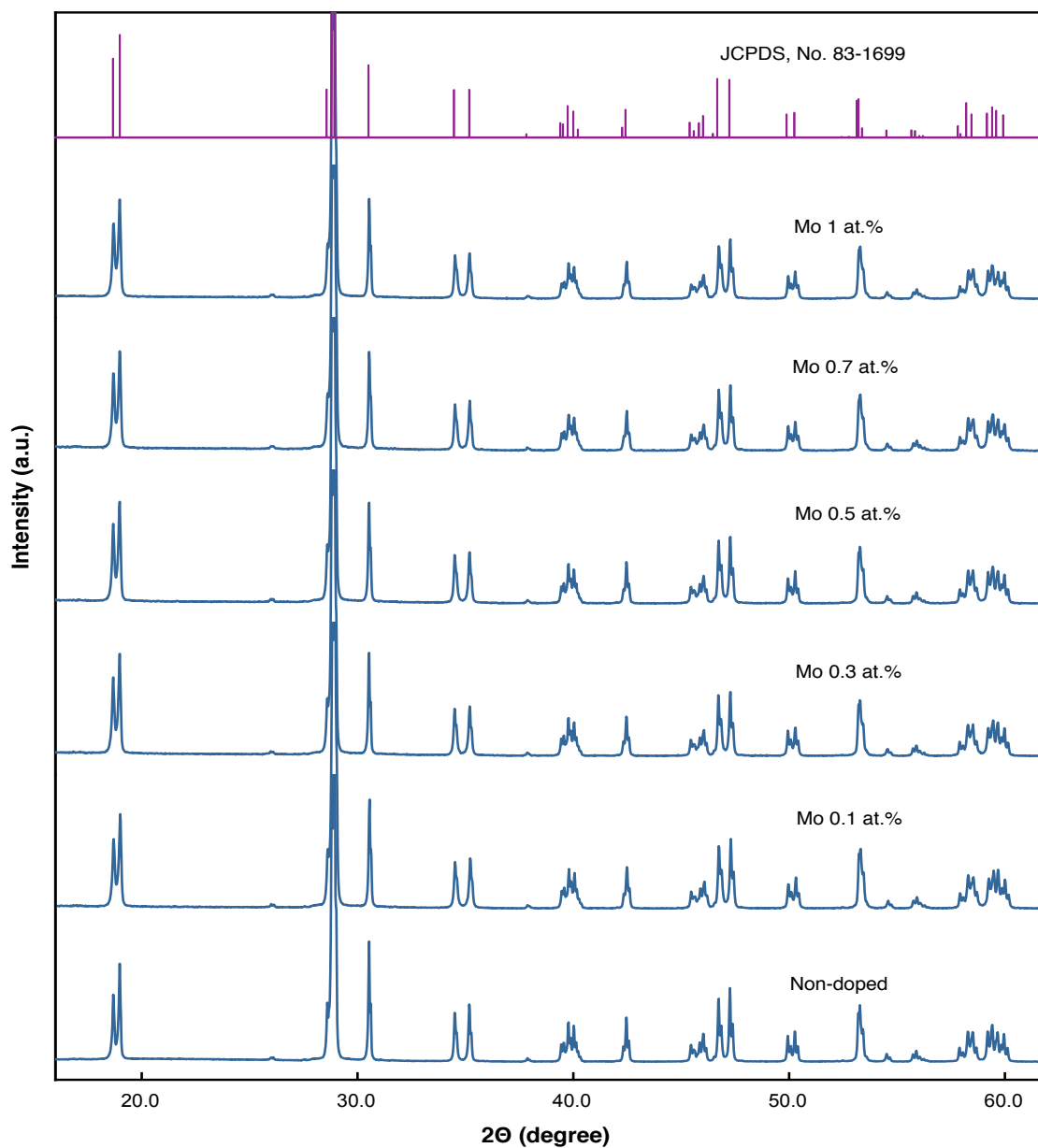
Supplementary Figure 3 | XRD patterns of as-synthesized BiVO<sub>4</sub> particles, BiVO<sub>4</sub> particles annealed at various temperatures, and BiVO<sub>4</sub> particles treated by 800 °C annealing followed with ball milling and 700 °C post-annealing. The reference XRD pattern of monoclinic BiVO<sub>4</sub> (JCPDS, No. 83-1699) is shown on the top.



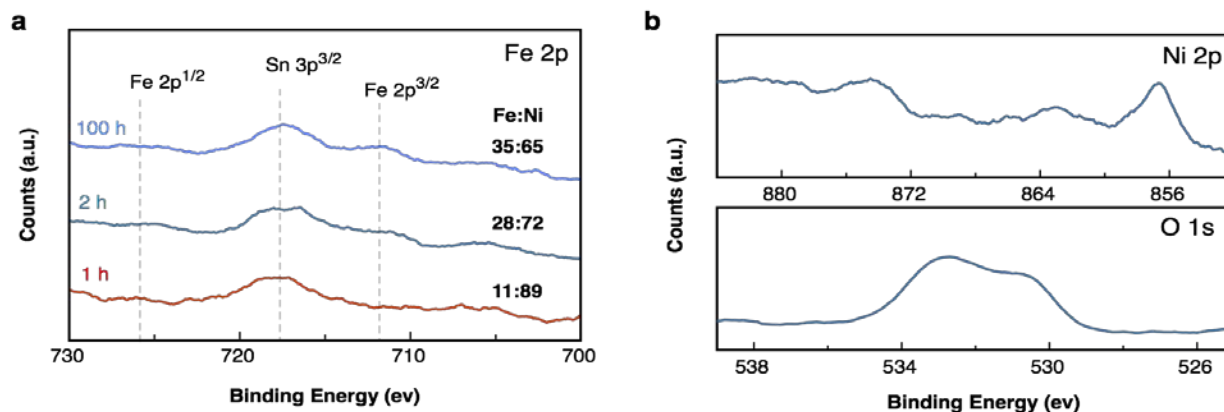
Supplementary Figure 4 | The corresponding current-time curves recorded in the absence of sulphite for the study of photocorrosion inhibition property shown in Figure 2. **a-b**, a nanoworm BiVO<sub>4</sub> electrode (a) and a 800°C-BM-700°C electrode (b) biased at 1.2 V vs. RHE under AM1.5G irradiation in 0.5 M pH 7 sodium phosphate buffer for 4 runs of 30 min treatment. The insets in (a) compare the photos of nanoworm electrodes taken before and after the two hour treatment, indicating significant loss of materials due to photo-induced electrochemical dissolution. **c**, a nanoworm BiVO<sub>4</sub> electrode biased at 0.6 V vs. RHE under AM1.5G irradiation in 0.5 M pH 7 sodium phosphate buffer for 4 runs of 30 min treatment. The improved photocurrents in run 2-4 are likely due to mild dissolution of BiVO<sub>4</sub> during run 1 that leads to the removal of surface states. **d**, a nanoworm BiVO<sub>4</sub> electrode biased at 1.2 V vs. RHE in dark in 0.5 M pH 7 sodium phosphate buffer for 2 runs of 1 hour treatment. The photocurrents for sulphite oxidation in 0.2 M sodium sulphite containing 1 M borate solution at pH 9 were recorded after each run for the electrodes, and the electrodes were pre-treated by scanning the potential (scan rate 40 mVs<sup>-1</sup>) between 0.15-1.25V vs. RHE for 5 cycles in the same sulphite solution under illumination before measurement.



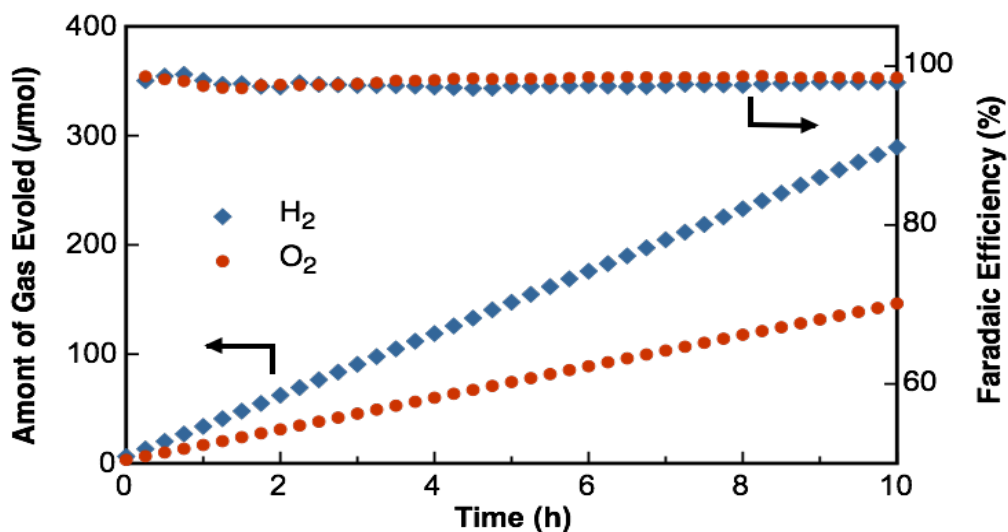
Supplementary Figure 5 | Photocorrosion behaviour of  $\text{BiVO}_4$  electrodes biased at a large overpotential for water oxidation. **a**, a bare  $800^\circ\text{C-BM-700}^\circ\text{C/Ni/Sn}$  electrode at 2 V vs RHE in dark in 0.5 M pH 7 sodium phosphate buffer. The inset compares the photocurrents for sulphite oxidation before and after the treatment. **b**, bare nanoworm  $\text{BiVO}_4$  electrodes at 2 V vs RHE in dark/light in 0.5 M pH 7 sodium phosphate buffer. The photo of the electrode taken after the treatment under AM1.5G irradiation and the comparison of sulphite oxidation photocurrents before and after the treatments are shown as the insets. Sulphite oxidation photocurrents were recorded in 1 M pH 9 potassium borate buffer containing 0.2 M sodium sulphite. The very high dark currents for water oxidation observed for  $800^\circ\text{C-BM-700}^\circ\text{C/Ni/Sn}$  electrode were due to the catalytic effect of Ni species in the contacting substrate. Since the PEC performance as indicated by sulphite oxidation photocurrents showed no change after the treatment in dark for both cases, the high applied voltage (or low fermi level of electrons) can therefore be ruled out as a direct cause for the corrosion observed in light. Under AM1.5G irradiation, the photocurrents within the first hour at 2 V vs RHE for nanoworm  $\text{BiVO}_4$  electrode were much higher than those at 1.2 V vs RHE (Supplementary Figure 5), which correlates well with the rate of performance drop and dissolution of  $\text{BiVO}_4$ .



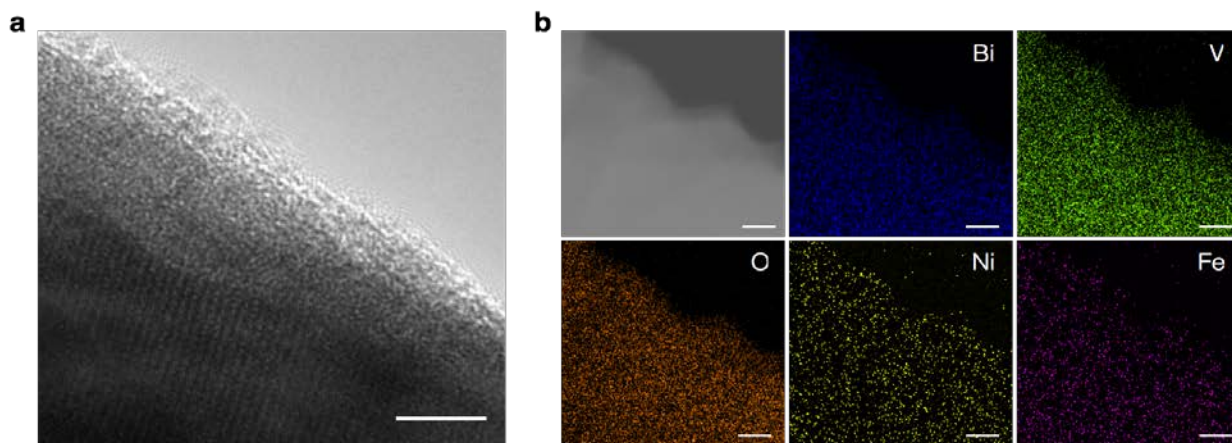
Supplementary Figure 6 | XRD patterns of BiVO<sub>4</sub> particles with various Mo doping concentrations (0-1 at.%). All BiVO<sub>4</sub> particles were treated by 800 °C annealing, ball milling and 700 °C post annealing sequentially. The reference XRD pattern of monoclinic BiVO<sub>4</sub> (JCPDS, No. 83-1699) is shown on the top.



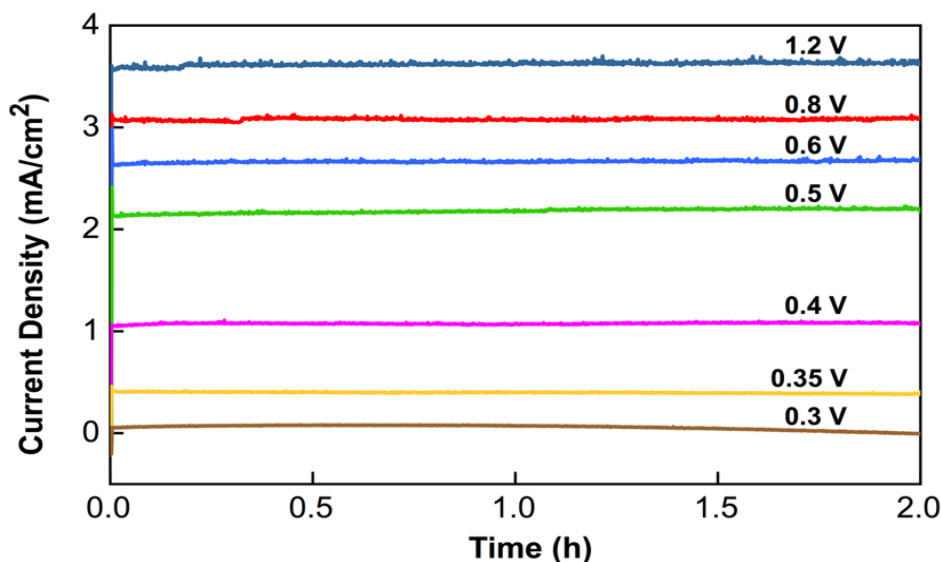
Supplementary Figure 7 | XPS spectra. **a**, comparison of Fe 2p XPS spectra for the Mo:BiVO<sub>4</sub>/Ni/Sn electrodes after 1 and 2 hour catalytic activation in fresh 1 M borate buffer (pH 9), and NiFe-OEC/Mo:BiVO<sub>4</sub>/Ni/Sn electrode after 100-hour water splitting at 0.6 V vs. RHE. The atomic percentages of Fe in the total metal content of the NiFe-OEC layer for the three samples were quantitatively determined by XPS to be 11%, 28% and 35% respectively. **b**, the corresponding Ni 2p and O 1s XPS spectra for the sample used after 100-hour water splitting.



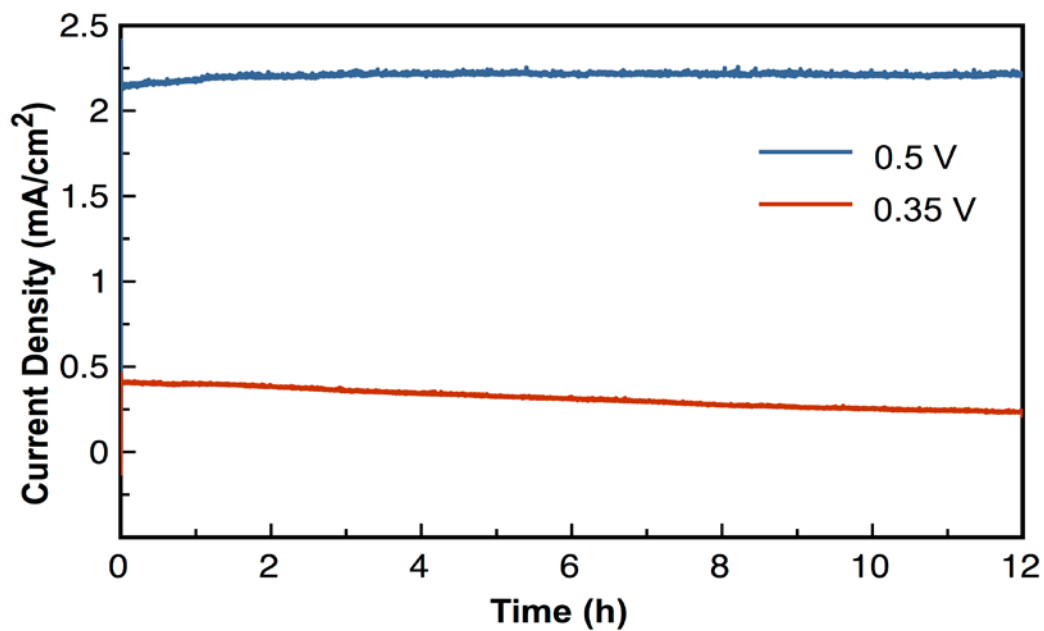
Supplementary Figure 8 | Gas evolutions and faradaic efficiency for catalytically activated NiFe-OEC/Mo:BiVO<sub>4</sub>/Ni/Sn electrode measured at 0.6 V vs. RHE by gas chromatography.



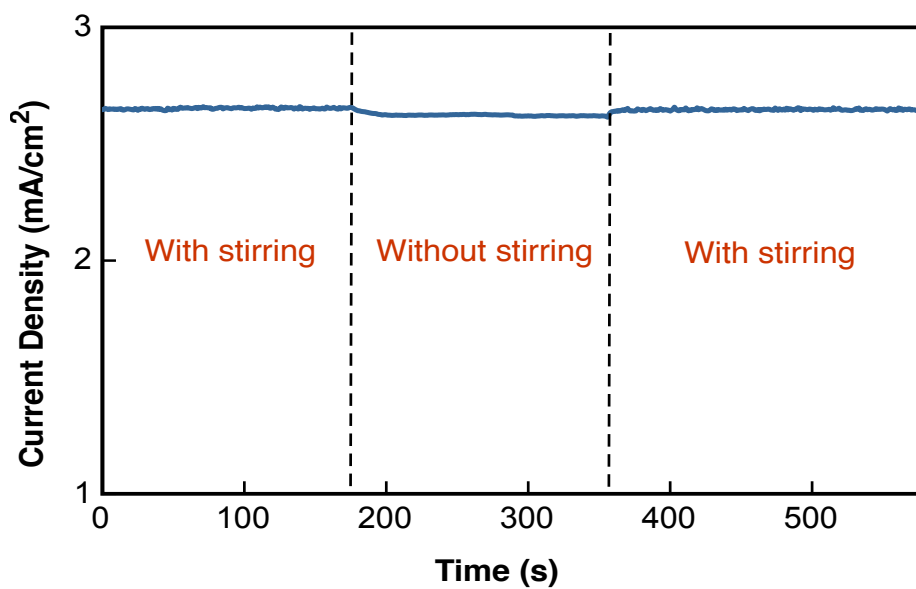
Supplementary Figure 9 | HRTEM image (a) and STEM-EDS elemental mapping images (b) of the  $\text{BiVO}_4$  particles from a NiFe-OEC/Mo:BiVO<sub>4</sub>/Ni/Sn electrode after 100-hour water splitting at 0.6 V vs. RHE. Scale bars: **a**, 4 nm; **b**, 20 nm.



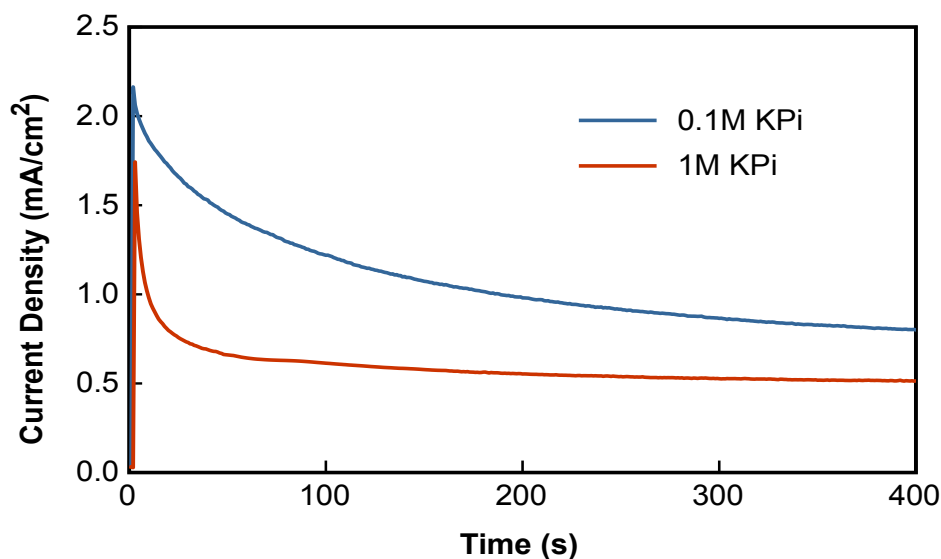
Supplementary Figure 10 | Effect of applied potential on the stability of NiFe-OEC decorated Mo:BiVO<sub>4</sub>/Ni/Sn electrodes. 2-hour water splitting stability measurements were conducted in the range of 0.3-1.2 V vs. RHE. Above 0.4 V vs. RHE, the electrode was stable at all tested potentials, which is an important feature if it is to be coupled with photocathodes with different working potentials. Below 0.4 V vs. RHE, BiVO<sub>4</sub>-based photoanodes are intrinsically unstable due to the reduction of V<sup>5+</sup> to V<sup>4+</sup>. The performance drop due to V<sup>5+</sup> reduction at 0.35 V vs. RHE became more obvious when compared with the stability at 0.5 V vs. RHE in a 12 hour test (Supplementary Figure 11).



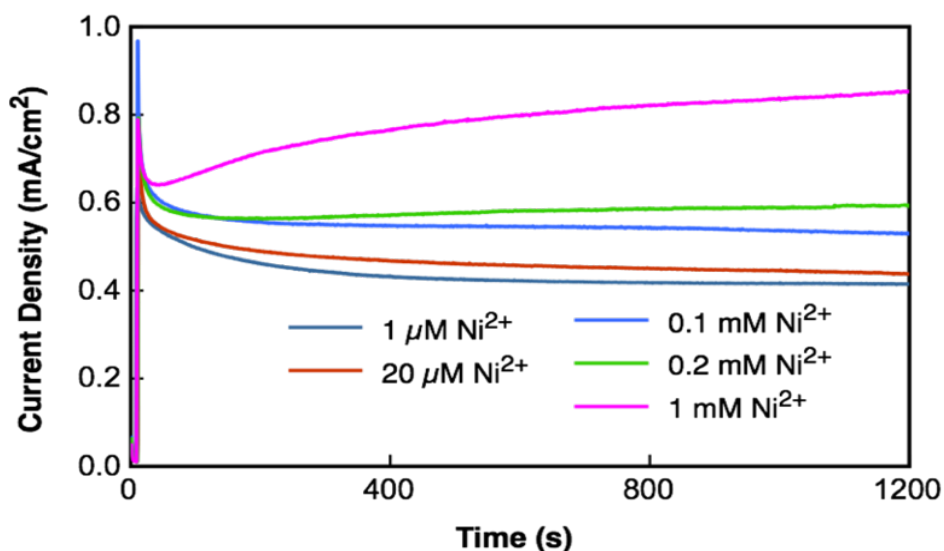
Supplementary Figure 11 | Comparison of 12-hour water oxidation stabilities at 0.35 V and 0.5 V vs. RHE in 1 M borate buffer for NiFe-OEC decorated Mo:BiVO<sub>4</sub>/Ni/Sn electrodes.



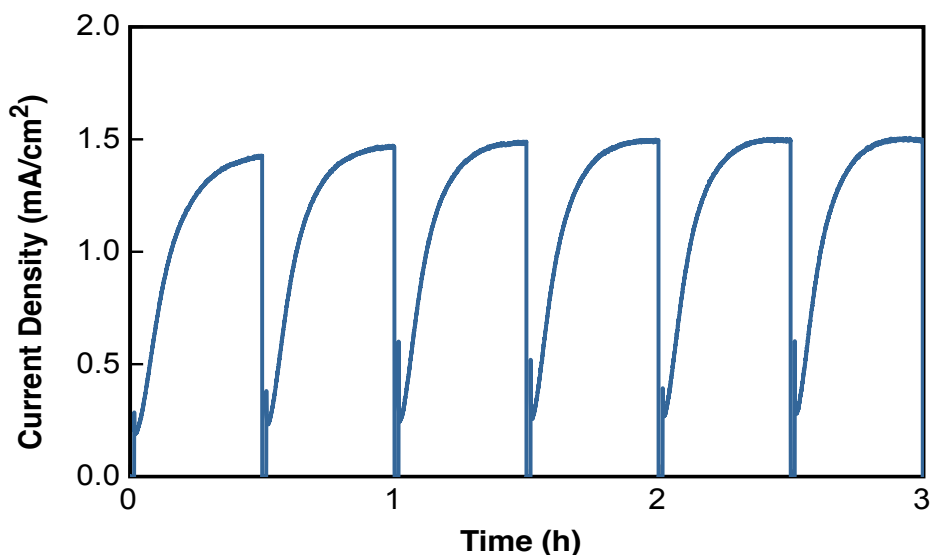
Supplementary Figure 12 | Comparison of photocurrents of NiFe-OEC/Mo:BiVO<sub>4</sub>/Ni/Sn electrode at 0.6 V vs. RHE with and without magnetic stirring in 1 M pH 9 borate buffer under simulated AM1.5G irradiation.



Supplementary Figure 13 | Stabilities of activated NiFe-OEC/Mo:BiVO<sub>4</sub>/Ni/Sn electrodes in 0.1 M and 1 M potassium phosphates (KPi) at pH 7 under simulated AM 1.5G irradiation with an applied bias of 1 V vs. RHE. The photocurrents of fully activated NiFe-OEC/Mo:BiVO<sub>4</sub>/Ni/Sn electrodes at 0.6 V vs. RHE drops very fast in a fresh 0.1 M potassium phosphate at pH 7, and even faster in more concentrated 1 M potassium phosphate. Complete dissolution of NiFe-OECs in 1 M potassium phosphate can be done within several minutes.



Supplementary Figure 14 | Dependence of Ni OEC deposition rate on Ni<sup>2+</sup> concentration in 1 M potassium phosphate at pH 7. J-t curves of bare Mo:BiVO<sub>4</sub>/Tn/Sn electrodes at 1 V vs. RHE in 1 M potassium phosphate buffer at pH 7 were measured with different concentrations of Ni<sup>2+</sup> ions from 1 μM to 1 mM. The changes of Ni<sup>2+</sup> concentration from 1 μM to 0.2 mM only showed the effect of retarding the decrease of photocurrent. Very slow increase in photocurrent was only observed with Ni<sup>2+</sup> concentration as high as 1 mM, which is 1000 times of the concentration used for Ni-OEC deposition in 1 M borate buffer.



Supplementary Figure 15 | Current-time curve of a bare Mo:BiVO<sub>4</sub>/Tn/Sn electrode in 10 μM Ni<sup>2+</sup> containing 1 M potassium phosphate at pH 9 under intermittent AM 1.5G irradiation. The irradiation was turned off for 1 minute after every 30 minutes. The Ni catalyst deposited on Mo:BiVO<sub>4</sub>/Ti/Sn electrode over 30-minute irradiation in 10 μM Ni containing solution almost completely dissolved in 1 minute in dark. Compared to the data shown in Supplementary Figure 14, increasing the pH of 1 M potassium phosphate from 7 to 9 can indeed improve the deposition rate of Ni, but still the dissolution of Ni-based catalyst is too fast for practical use.